ELSEVIER

PII: S0032-3861(96)00769-0

Polymer Vol. 38 No. 9, pp. 2183–2189, 1997
© 1997 Elsevier Science Ltd
Printed in Great Britain. All rights reserved
0032-3861/97/$17.00 + 0.00

Real-time monitoring of swelling and dissolution of poly(methyl methacrylate) discs using fluorescence probes

Ö. Pekcan*, Ş. Uğur and Y. Yılmaz
Department of Physics, Istanbul Technical University, 80626, Maslak-Istanbul, Turkey
(Received 19 February 1996; revised 3 May 1996)

A new technique, based on steady state fluorescence measurements is introduced for studying swelling and dissolution of polymer discs. These discs are formed by free radical polymerization of methyl methacrylate (MMA). Pyrene (Py) was introduced as a fluorescence probe during polymerization. Swelling and dissolution of disc shape poly(methyl methacrylate) (PMMA) samples in chloroform–heptane mixtures were monitored in real-time by the Py fluorescence intensity change. The effects of solvent quality and agitation (stirring) on film dissolution were studied. Sorption and desorption coefficients of solvent and Py molecules were measured respectively during dissolution of films, and found to be between 10^{-7} and 10^{-6} cm^2 s^{-1}. © 1997 Elsevier Science Ltd.

(Keywords: fluorescence; gel; diffusion; dissolution; relaxation; swelling)

INTRODUCTION

The dissolution of glassy polymer films can be divided into three steps. The first is the diffusion of solvent molecules into the polymer matrix. In the second step, the solvent molecules initiate the relaxation of polymer chains and a solvent swollen gel is formed. The third and the final step consists of diffusion of polymer chains from the gel into the solvent reservoir. A schematic representation of these three sequential steps for the dissolution of a glassy polymer film is shown in *Figure 1*.

The penetration of solvent molecules into glassy polymers often does not proceed according to the Fickian diffusion model[1,2]. Penetration not described by the Fickian model is called anomalous diffusion, where the rate of transport is entirely controlled by polymer relaxations. This transport mechanism is termed case II in contrast to Fickian diffusion which is called case I. In the case II diffusion model, the second step is the rate limiting step which predicts a linear dependence of the change in film thickness on time. The first and third steps, however, follow a case I diffusion model, where the first one is the sorption of solvent molecules by the glassy film and the third is the desorption of polymer chains from the gel layer (see *Figure 1*).

Solvent penetration in polymers has been studied by various techniques. The most traditional ones are the weight measurements and monitoring the redistribution of isotopic tracers in the polymer[3]. The electron spin resonance (e.s.r.) technique was used to investigate non-solvent penetration into poly(methyl methacrylate) (PMMA) latex particles[4]. E.s.r. method based on the scavenging of radicals produced by high energy γ-irradiation of PMMA by oxygen was used for the measurement of diffusion coefficients in PMMA[5]. Penetration of naphthalene molecules into PMMA latex particles, stabilized by polyisobutylene (PIB) was studied by a time resolved fluorescence technique, below T_g[6]. Fluorescence quenching and depolarization methods have been used for penetration and dissolution studies in solid polymers[7–9]. *In-situ* fluorescence quenching experiments in conjunction with laser interferometry were used to investigate dissolution of PMMA film in various solvents[10]. The real-time, nondestructive method for monitoring small molecule diffusion in polymer films was developed[11,12]. This method is basically based on the detection of excited fluorescence molecules desorbing from a polymer film into a solution in which the film is placed[11–14]. Recently, we have reported a steady state fluorescence (SSF) study on dissolution of annealed latex films using real-time monitoring of fluorescence probes[15].

Polymer dissolution processes can be affected by various parameters, including solvent quality, polymer molecular weight, solvent thermodynamic compatibility, agitation and temperature. In this work, the effect of solvent quality and agitation to polymer dissolution process were studied using the SSF method by real-time monitoring of the pyrene (Py) intensity change. Chloroform and heptane mixtures are used as dissolution agents. *In-situ* SSF experiments are performed to observe the swelling and dissolution processes. Swelling experiments were carried out by illuminating only the PMMA film, so that unquenched Py molecules were monitored in real time. Dissolution experiments were designed so that Py molecules, desorbing from swollen gel, are detected in real time monitoring of SSF intensity. In order to do this, direct illumination of the disc sample is avoided, during the *in-situ* dissolution experiment.

* To whom correspondence should be addressed

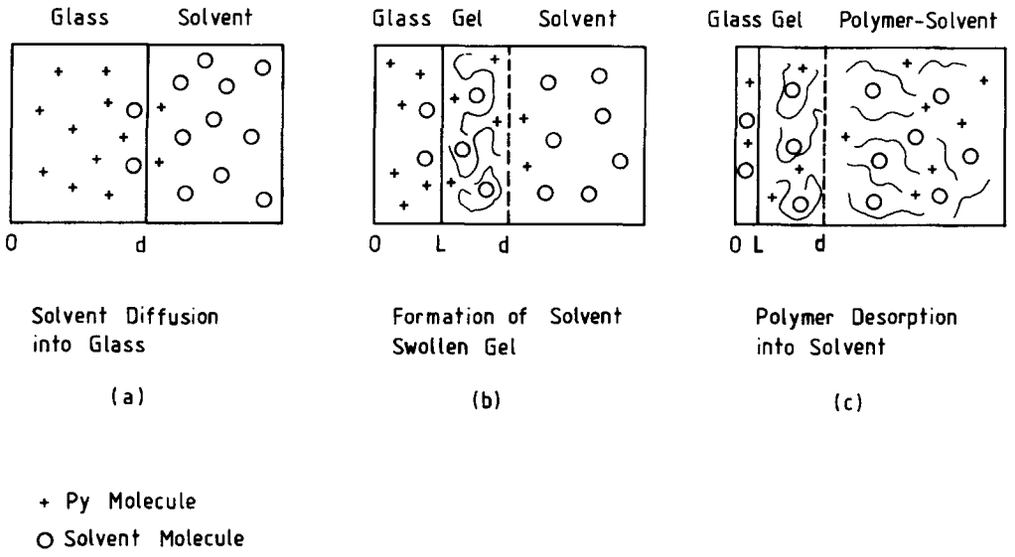

Figure 1 Scheme of polymer film dissolution. d is the film thickness and L is the position of the advancing gel front. Py and solvent molecules are also presented

THEORETICAL CONSIDERATION

Various mechanisms and various mathematical models have been considered for the polymer dissolution. Quano[16] proposed a model which includes a polymer diffusion in a liquid layer adjacent to the polymer and moving of the liquid-polymer boundary. The key parameter for this model was the polymer disassociation rate, defined as the rate at which polymer chains desorb from the gel interface. Peppas[17] extended this model for films to the situation of the polymer dissolution rate where gel thickness was found to be proportional to $(\text{time})^{1/2}$. A relaxation controlled model was proposed by de Gennes and Brochard[18] where, after a swelling gel layer was formed, desorption of polymer from the swollen bulk was governed by the relaxation rate of the polymer stress. This rate was found to be of the same order of magnitude as the reptation time. The dependences of the radius of gyration and the reptation time on polymer molecular weight and concentration were studied, using a scaling law[19], based on the reptation model.

In this paper, we employed a simpler model, developed by Enscore *et al.*[1] to interpret the results of polymer swelling and dissolution experiments. This model includes case I and case II diffusion kinetics.

Case I or Fickian diffusion

The solution of a unidirectional diffusion equation for a set of boundary conditions is cited by Crank[3]. For a constant diffusion coefficient, D and fixed boundary conditions, the sorption and desorption transport in and out of a thin slab is given by the following relation

$$\frac{M_t}{M_\infty} = 1 - \frac{8}{\pi^2}\sum_{n=0}^{\infty}\frac{1}{(2n+1)^2}\exp\left(\frac{-(2n+1)^2 D\pi^2 t}{d^2}\right) \quad (1)$$

Here, M_t represents the amount of materials absorbed or desorbed at time t, M_∞ is the equilibrium amount of material, and d is the thickness of the slab.

Case II diffusion

Case II transport mechanism is characterized by the following steps. As the solvent molecules enter into the polymer film, a sharp advancing boundary forms and separates the glassy part from the swollen gel (see *Figure 1b*). This boundary moves into the film at a constant velocity. The swollen gel behind the advancing front is always at a uniform state of swelling. Now, consider a cross-section of a film with thickness d, undergoing Case II diffusion as in *Figure 1*, where L is the position of the advancing sorption front, C_0 is the equilibrium penetrant concentration and k_0 ($\text{mg cm}^{-2}\,\text{min}^{-1}$) is defined as the Case II relaxation constant. The kinetic expression for the sorption in the film slab of an area A is given by

$$\frac{dM_t}{dt} = k_0 A \quad (2)$$

The amount of penetrant, M_t absorbed in time t will be

$$M_t = C_0 A(d - L) \quad (3)$$

After equation (3) is substituted into equation (2) the following relation is obtained

$$\frac{dL}{dt} = -\frac{k_0}{C_0} \quad (4)$$

It can be seen that the relaxation front, positioned at L, moves toward the origin with a constant velocity, k_0/C_0. The algebraic relation for L, as a function of time t, is described by equation (5):

$$L = d - \frac{k_0}{C_0}t \quad (5)$$

Since $M_t = k_0 A t$ and $M_\infty = C_0 A d$, the following relation is obtained

$$\frac{M_t}{M_\infty} = \frac{k_0}{C_0 d}t \quad (6)$$

EXPERIMENTAL

The radical polymerization of MMA was performed in bulk in the presence of 2,2′-azobisisobutyronitrile (AIBN) as an initiator. AIBN (1.59×10^{-2} M) and Py (4×10^{-4} M) were dissolved in MMA and this solution was transformed into round glass tube of 15 mm internal diameter. Before polymerization, each solution was deoxygenated by bubling nitrogen for 10 min. Radical polymerization of the MMA was performed at 65 ± 3°C.

After polymerization was complete the tube was broken. Disc-shaped, thin samples (around 0.2 cm) were cut for the swelling and dissolution experiments.

The monomers MMA (Merck) were freed from the inhibitor by shaking with a 1.79 M aqueous KOH solution, washing with water and drying over sodium sulfate. They were then distilled under reduced pressure over copper chloride. The initiator, AIBN (Merck) was recrystallized twice from methanol. The solvents chloroform and heptane (Merck) were used as they are received.

In situ fluorescence experiments were performed using a Perkin Elmer LS-50 spectrofluoremeter. All measurements were made at the 90° position and the slit widths were kept at 2.5 mm. Swelling experiments were performed in a 1 × 1 cm quartz cell which was placed in the spectrofluorimeter. The fluorescence emission was monitored so that only the disc sample was illuminated by the excitation light. Disc shape samples were placed at one side of a quartz cell filled with chloroform–heptane mixture and samples were then illuminated with 345 nm excitation light. The pyrene fluorescence intensity, I_p, was monitored during the swelling process at 375 nm using the 'time drive' mode of the spectrofluorimeter. Emission of Py was recorded continuously at 375 nm as a function of time. The cell and the sample position are presented in *Figure 2a*.

Dissolution experiments were carried out as described above except that the film samples were shifted to the upper side of the quartz cell, so that samples were not illuminated by the excitation light. Here the 1 × 1 cm quartz cell was equipped with a magnetic stirrer at the bottom. The Py fluorescence emission was monitored at a 90° angle as shown in *Figure 2b*.

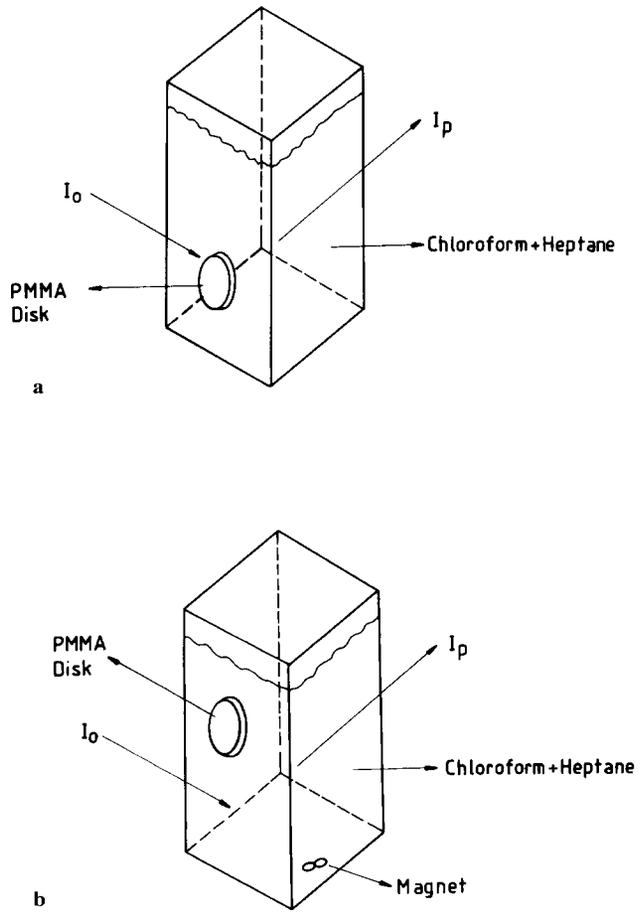

Figure 2 Dissolution cell as used in the LS-50 Perkin–Elmer Spectrofluorimeter for (a) swelling and (b) dissolution experiments. I_0 and I_p are the excitation and emission intensities at 345 nm and 375 nm respectively

RESULTS AND DISCUSSION

Dissolution with stirrer

Dissolution experiments were first performed by using solely chloroform as a dissolution agent. *Figure 3*

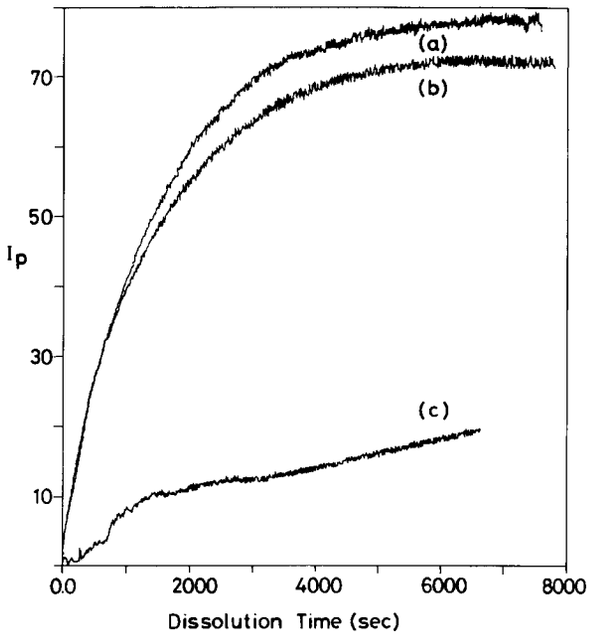

Figure 3 Pyrene intensity, I_p vs dissolution time for the three different experiments. *a*, *b* and *c* indicate the curves for high, low and no magnetic stirrer speeds. The cell was illuminated at 345 nm, as shown in *Figure 2b*, during fluorescence measurements

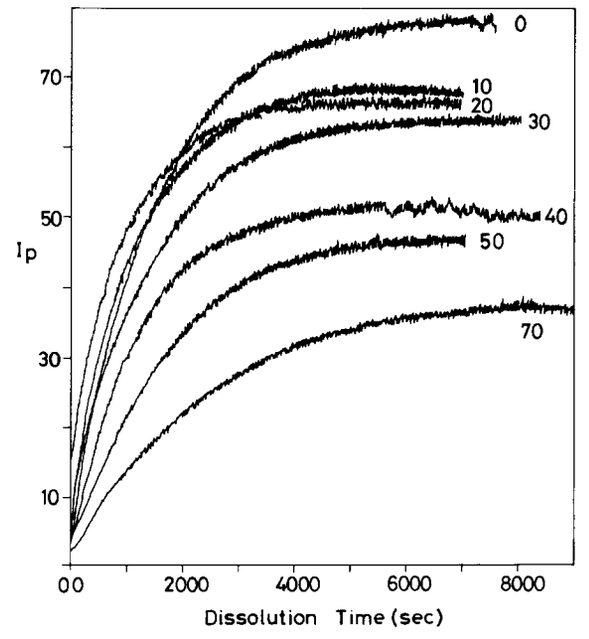

Figure 4 Pyrene intensity, I_p vs dissolution time for the film samples dissolved in various chloroform–heptane mixtures at high stirring speed. Numbers above the curves indicate the percents of heptane content

presents the plot of Py intensity, I_p vs dissolution time where *a* and *b* represent the curves at high and low speeds of magnetic stirrer respectively. Dissolution curve with no magnetic stirrer is shown with *c* in *Figure 3*. For high and low stirring speeds, the asymptotic values of the dissolution curves are reached by following the case I diffusion model. On the other hand, in the same time interval, dissolution curve for no stirrer presents linear behaviour after a short delay which may obey case II model. These results indicate that dissolution processes are strongly affected by agitation (stirring). In this work, first we carried out dissolution experiments with high stirring speeds. Also, swelling and dissolution processes were studied with no stirring.

Dissolution curves for various chloroform–heptane mixtures at high stirring speed are shown in *Figure 4*. It is seen that, as the heptane content increases, curves reach a plateau at later times. In other words, PMMA films dissolve slower in higher heptane content solutions. In order to understand the smaller intensity values at higher heptane content samples, SSF spectra of Py were taken in various chloroform–heptane mixtures. *Figure 5* presents the results for the samples of 10, 30 and 70% heptane content mixtures. No shift is observed at the maximum Py intensity. Smaller intensity values in Py spectra for high heptane content mixture can be explained by the low viscosity (3.8×10^{-4} Pa s) effect of heptane, in which excited Py can be quenched much easier than is possible with a high chloroform (5.8×10^{-4} Pa s) content mixture[20].

The curves in *Figure 4* seem to follow a case I (Fickian) diffusion model. In processing the dissolution data, it is assumed that I_p is proportional to the number of Py molecules desorbing from the PMMA film. The logarithmic form of equation (1) is written for $n = 0$, with $A_d = D_d\pi^2/d^2$ and $B_d = \ln(8/\pi^2)$, as follows

$$\ln(1 - I_p/I_{p_\infty}) = B_d - A_d t \qquad (7)$$

Here, I_{p_∞} presents the number of Py molecules at the equilibrium condition, D_d is the desorption coefficient and *d* is the thickness of the PMMA disc. *Figures 6a–c* show dissolution curves for 10, 30 and 70% heptane content mixtures, which are digitized for numerical treatment according to equation (7). All curves in *Figure 6* present linear dependences on time, confirming our assumption of relationship with a diffusion model.

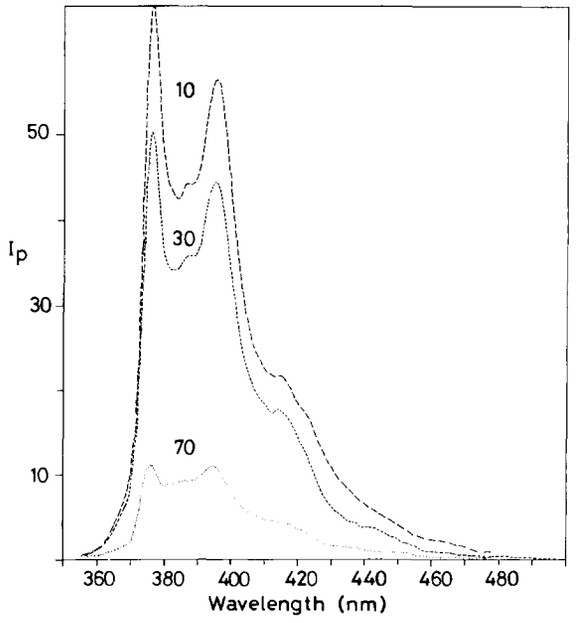

Figure 5 Emission spectra of Pyrene (Py) in 10, 30 and 70% heptane content mixtures

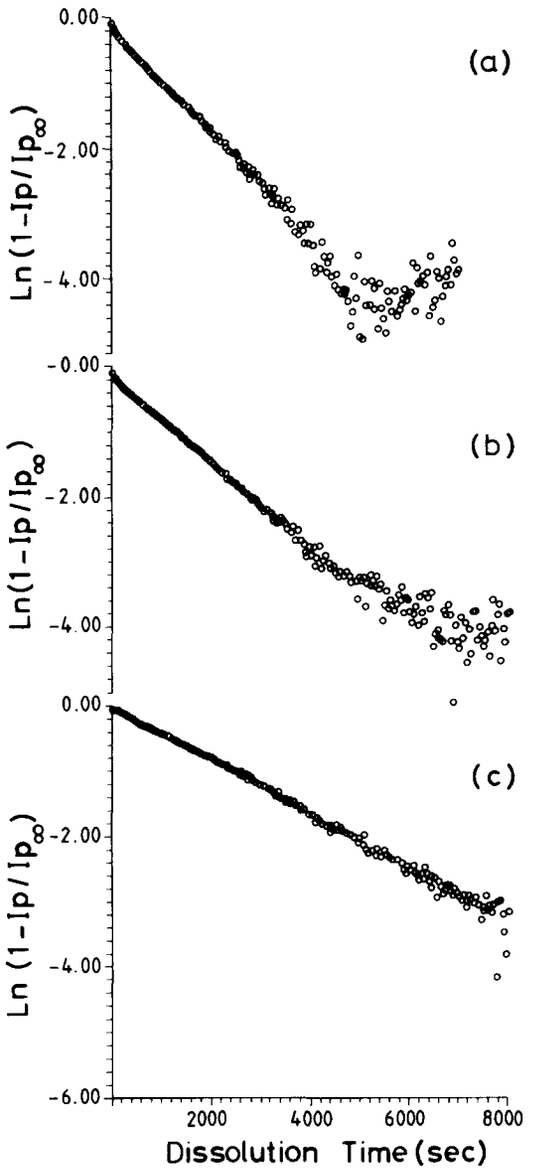

Figure 6 Plot of digitized data of *Figure 4*, which obey the relation $\ln[1 - (I_p/I_{p_\infty})] = B_d - A_d t$ where *t* is the dissolution time. *a*, *b* and *c* represent the data for 10, 30 and 70% heptane content samples

Table 1 D_d values were obtained by fitting equation (7) to the data in *Figure 4*. Here chloroform–heptane mixtures are used as dissolution agents and high speed stirring was employed during experiments. *d* represents the film thickness for each sample

Chloroform	Heptane	$\times 10^{6}$ D_d ($cm^2\ s^{-1}$)	*d* (cm)
100	0	3.73	0.196
90	10	2.81	0.182
80	20	3.48	0.191
70	30	1.93	0.169
60	40	2.81	0.206
50	50	2.25	0.185
30	70	1.59	0.233

When these linear curves in *Figures 6a–c* are compared to computations using equation (7), desorption coefficients, D_d, for Py molecules are obtained. These are listed in *Table 1* with values for other samples. Linear regression of the data in *Figures 6a–c* are presented as *Figures 7a–c* respectively. D_d values for the PMMA discs, dissolved in high heptane content mixtures, presented smaller values than did low heptane mixtures. This result is expected for PMMA dissolved in the solvent content mixture which contained a greater amount of the non-solvent. The plot of D_p *versus* heptane content is shown in *Figure 8*. Here, the straight line cuts the horizontal axis at 100% (pure heptane) at which $D_p = 0$, as expected.

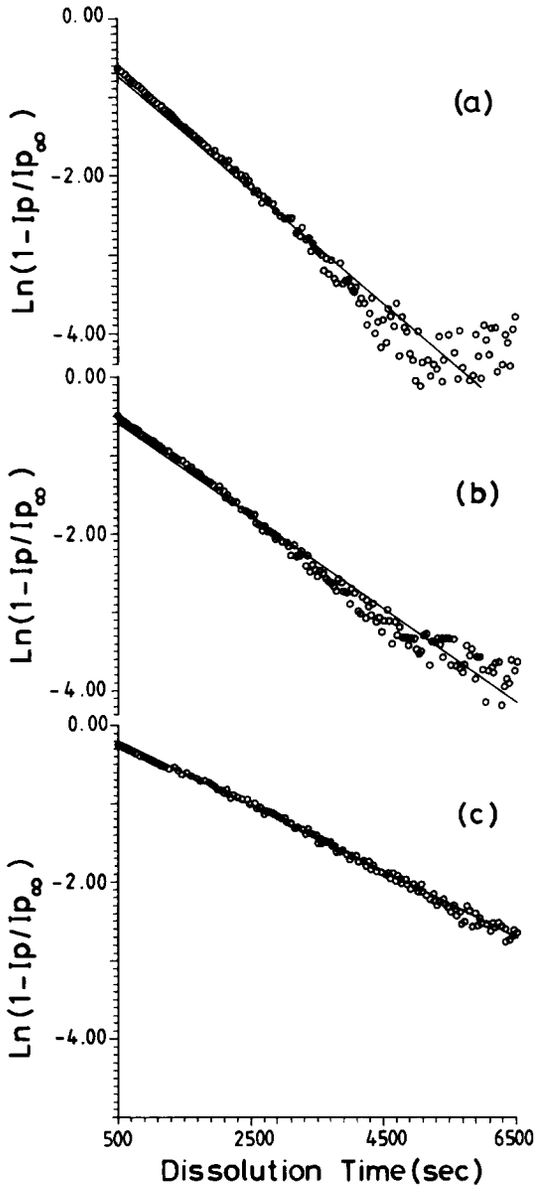

Figure 7 Comparison of the linear portions of the data presented in *Figures 6a–c* with the computations using equation (7). Desorption coefficients, D_d are obtained from the slopes of the plots in *a*, *b* and *c*

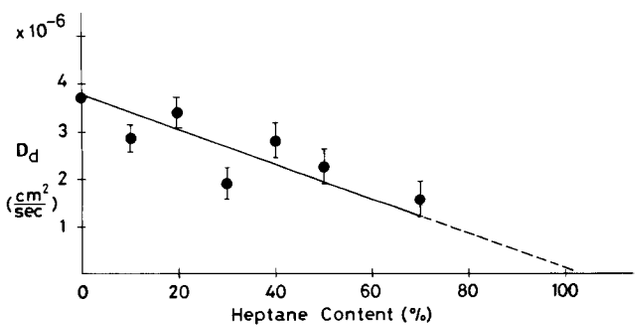

Figure 8 Plot of desorption coefficients, D_p *versus* heptane content (%) for the samples dissolved in chloroform–heptane mixtures

In general, D_d values obtained in these experiments are three orders of magnitude larger than that which was found in our recent work with PMMA latex films[15]. In this study the PMMA discs were 200 times thicker than the latex films. Thickness effects are observed by Enscore *et al.*[1] where 300 times larger polystyrene spheres caused two times larger desorption coefficients for hexane. This was explained by formation of the spherical shell during sorption process. In our case, however, the gel layer is removed from the surface of the PMMA disc by the stirring effect. Smaller desorption coefficients in latex films compared to those of PMMA discs can be explained by the annealing effect, which resulted in the formation of mechanically strong films. Most probably, PMMA discs used in this work may have greater free volumes than have the annealed latex films. In fact, during latex film dissolution, a long gelation period (case II diffusion) was observed at early times. However, the PMMA discs used here present dissolution by following pure Fickian (case I) behaviour.

Swelling and dissolution without stirrer

Figure 9 gives the results of swelling experiments which are performed by illuminating only the film samples by the excitation light. Two different experiments, with pure chloroform and 40% heptane content mixture were carried out and I_p monitored with time. It can be seen in *Figure 9* that values of I_p decrease exponentially as the

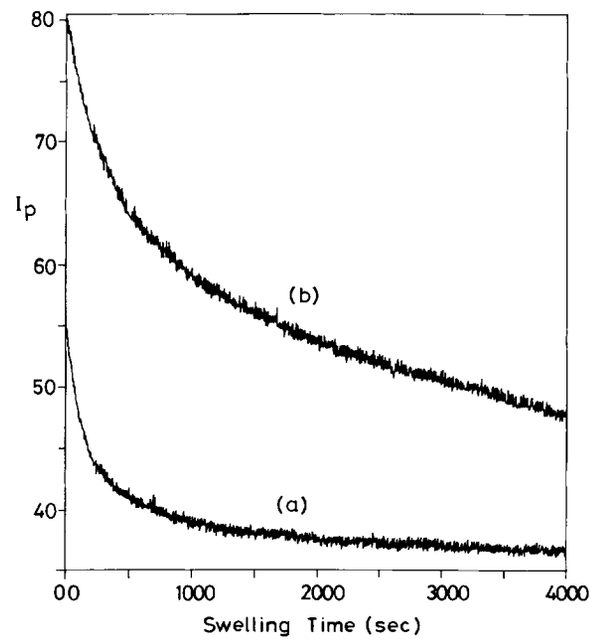

Figure 9 Pyrene emission intensity, I_p vs swelling time for the film samples placed in (a) pure chloroform and (b) 40% heptane content mixture. The cell was illuminated at 345 nm as shown in *Figure 2a*, during fluorescence measurements

time increases, i.e. as solvent molecules penetrate into the PMMA film. The excited Py molecules start to quench and, as a result, I_p decreases with increasing time. The quenching mechanism has been well documented in this field. It is known that interactions between the chromophore and the solvent molecule effect the energy difference between the ground and excited states[20]. It was reported that fluorescence intensities of aromatic molecules are affected by both radiative and non-radiative processes[21]. If the possibility of perturbation due to oxygen is excluded, the radiative probabilities are found to be relatively independent of the environment and even of the molecular species. Environmental effects on non-radiative transitions, which are primarily intra-molecular in nature, are believed to arise from break down of the Born–Oppenheimer approximation[22]. The role of the solvent in such a picture is to add the quasi-continuum of states needed to satisfy energy resonance conditions. The solvent acts as an energy sink for rapid vibrational relaxation which occurs after the rate limiting transition from the initial state. Recently, we have reported viscosity effects on low frequency, intra-molecular vibrational energies of excited naphthalene in swollen PMMA latex particles[20].

The results in *Figure 9* can be quantified by assuming that, I_p decreases as M_t increases, obeying case I model, according to the following relationship[5]

$$\frac{M_t}{M_\infty} = \left(1 - \frac{I_p}{I_{0p}}\right) \tag{8}$$

Here I_{0p} presents the initial value of the I_p intensity. Using equations (1) and (8) one can obtain the useful equation

$$\ln(I_p/I_{0p}) = B_s - A_s t \tag{9}$$

with $B_s = \ln(8/\pi^2)$ and $A_s = D_s\pi^2/d^2$, where D_s is the sorption coefficient and d is the initial thickness of the PMMA discs. The Fickian part of the data in *Figure 9* is digitized and plotted in *Figure 10* according to equation (9). Linear regression of the curves in *Figure 10* produces D_s coefficients, which are listed in *Table 2*. D_s is found to be larger in pure chloroform ($3.25 \times 10^{-7}\,cm^2\,s^{-1}$) than in the heptane mixture ($2.05 \times 10^{-7}\,cm^2\,s^{-1}$). This is understandable due to bad solubility of heptane in PMMA. Here one should notice that the sorption coefficients, D_s acquired without stirring are an order of magnitude smaller than the desorption coefficients, D_d acquired with stirrer. Here we have to note that swelling curves cannot be obtained in the stirring experiments, presumably due to fast sorption processes.

Dissolution curves, occurring without stirring being applied, for pure chloroform and for the 40% heptane content mixture are shown in *Figures 11a* and *b* respectively. These curves are obtained by direct

Table 2 D and k_0 values were obtained by fitting equation (9) and equation (10) to the data in *Figure 9* and *Figure 11*. Two different solvent mixtures were used as dissolution agents and no stirrer was used during these experiments

Chloroform	Heptane	$\times 10^{-7}$ D_s ($cm^2\,s^{-1}$)	k_0 ($mg\,cm^{-2}\,min^{-1}$)	d (cm)
100	0	3.25	7.35	0.205
60	40	2.07	1.85	0.189

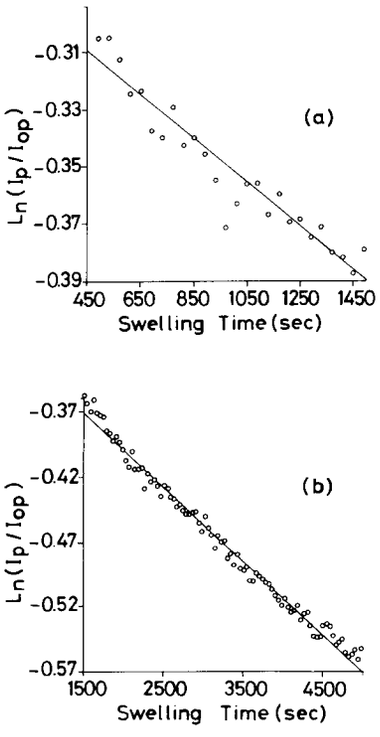

Figure 10 Comparison of the linear portions of the data presented in *Figures 9a* and *b* with the computations using equation (9). Sorption coefficients, D_s are obtained from the slopes of the plots in (a) and (b), for the film samples placed in pure chloroform and 40% heptane content mixture respectively

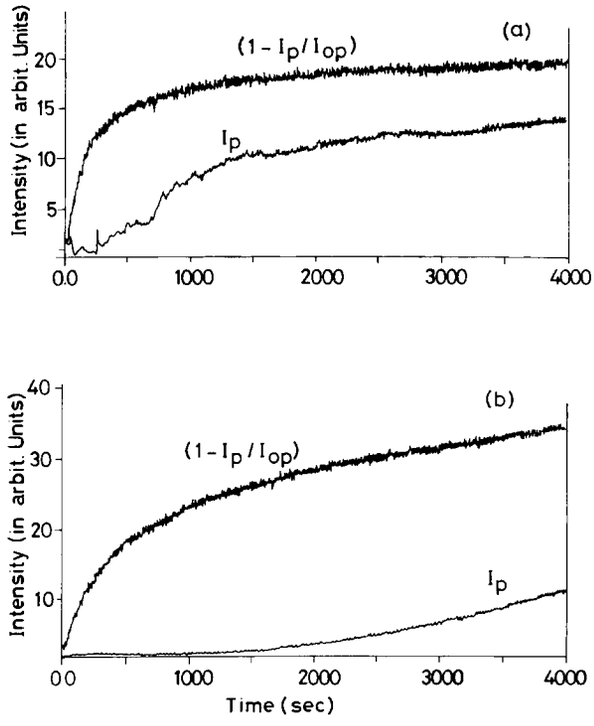

Figure 11 $(1 - I_p/I_{0p})$ (i.e. solvent sorption, M_t/M_∞) are compared with the dissolution curves (I_p) for the film samples dissolved in (a) pure chloroform and (b) 40% heptane content mixture. The cell was illuminated at 345 nm as shown in *Figure 2b* except no stirrer was used during fluorescence measurements

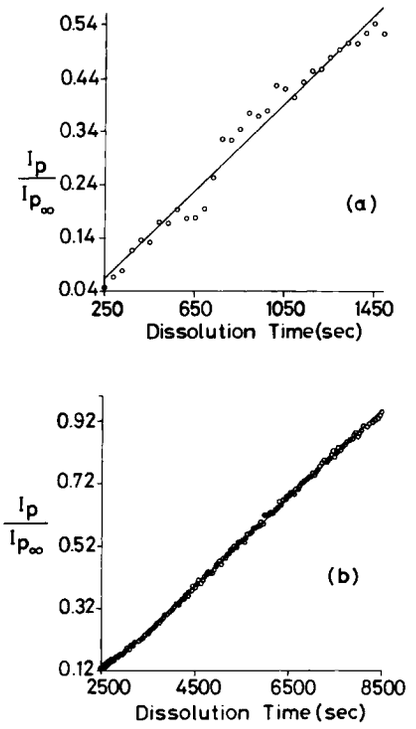

Figure 12 Comparison of the dissolution data presented in *Figures 11a* and *b* with the computations using equation (10). Relaxation constants, k_0 are obtained from the slopes of the plots in (a) and (b) for the films dissolved in pure chloroform and 40% heptane content mixture

illumination of solution in the fluorescence cell as shown in *Figure 2b*, except with no stirrer. $(1 - I_p/I_{0p})$ and dissolution curves (I_p) are compared in *Figure 11*, and certain delay can be observed between them. In fact dissolution starts after the swelling process is almost completed, i.e. the swollen gel layer is formed. Here it has to be noted that according to equation (8), $(1 - I_p/I_{0p})$ curves correspond to the solvent sorption (M_t/M_∞) in *Figure 11*. One may argue that the dissolution curves present the second step of the dissolution process, which obeys a case II diffusion model. Equation (6) can be used to quantify the dissolution data in *Figure 11* and can be written as

$$I_p/I_{p_\infty} = \frac{k_0}{C_0 d} t \qquad (10)$$

Linear regressions of the dissolution data in *Figures 11a* and *b* are presented in *Figures 12a* and *b*. These produced k_0 values from the slope of the curves. k_0 values, listed in *Table 2*, present larger values for pure chloroform than did the 40% heptane mixture, which can be explained again by the low solubility of heptane in PMMA. The measured k_0 values (7.35 and 1.85 mg cm^{-2} min^{-1}) in this work are an order of magnitude larger than those obtained for the latex films ($1–3 \times 10^{-1}$ mg cm^{-2} min^{-1})[15]. This difference can be explained by the annealing effect occurring during latex film formation which caused a stronger mechanical environment for the relaxing polymer chains.

CONCLUSION

In these fluorescence experiments we have shown that if no agitation (stirring) is present, film dissolution occurs according to a case II diffusion model and that solvent uptake (sorption) follows a case I diffusion model. In other words, as solvent molecules penetrate into a glassy polymer, a gel layer forms with time according to a case I model. In the meantime, the gel layer decreases in magnitude with time due to desorption of polymer chains according to a case II model. On the other hand in the presence of stirring pure Fickian (case I) behaviour is observed. This suggest that no gel layer can be formed at the surface of the glassy film during dissolution, i.e. the gel layer is taken off rapidly due to the effects of high stirring. In this case, sorption of solvent molecules is immediately followed by desorption of polymer chains from the swollen gel layer.

REFERENCES

1 Enscore, D. J., Hopfenbergand, H.B. and Stannett, V. T. *Polymer* 1977, **18**, 793
2 Thomas, N. L. and Windle, A. H. *Polymer* 1982, **23**, 529
3 Crank, J. and Park, G. S. 'Diffusion in Polymers', Academic Press, London, 1968
4 Veksli, Z. and Miller, W. G. *J. Polym. Sci.* 1976, **54**, 299
5 Kaptan, Y., Pekcan, Ö and Güven, O. *J. Appl. Polym. Sci.* 1989, **37**, 2537
6 Pekcan, Ö. *J. Appl. Polym. Sci.* 1993, **49**, 151
7 Guillet, J. E. in 'Photophysical and Photochemical Tools in Polymer Science' (Ed. M. A. Winnik), Reidel, Dordrecht, 1986
8 Nivaggioli, T., Wang, F. and Winnik, M. A. *J. Phys. Chem.* 1992, **96**, 7462
9 Pascal, D., Duhamel, J., Wang, Y., Winnik, M. A., Napper, D. H. and Gilbert, R. *Polymer* 1993, **34**, 1134
10 Limm, W., Dimnik, G. D., Stanton, D., Winnik, M. A. and Smith, B. A. *J. Appl. Polym. Sci.* 1988, **35**, 2099
11 Lu, L. and Weiss, R. G. *Macromolecules* 1994, **27**, 219
12 Kronganz, V. V., Mooney, W. F., Palmer, J. W. and Patricia, J. J. *J. Appl. Polym. Sci.* 1995, **56**, 1077
13 Kronganz, V. V. and Yohannan, R. M. *Polymer* 1990, **31**, 1130
14 He, Z., Hammond, G. S. and Weiss, R. G. *Macromolecules* 1992, **25**, 501
15 Pekcan, Ö., Canpolat, M. and Kaya, D. *J. Appl. Polym. Sci.* 1996, **60**, 2105
16 Tu, Y. O. and Quano, A. C. *IBM J. Res. Dev.* 1977, **21**, 131
17 Lee, P. I. and Peppas, N. A. *J. Controlled Release* 1987, **6**, 207
18 Brochardt, F. and de Gennes, P. G. *Physico. Chem. Hydrodynamics* 1983, **4**, 313
19 Papanu, J. S., Soane, D. S. and Bell, A. T. *J. Appl. Polym. Sci.* 1989, **38**, 859
20 Pekcan, Ö. *J. Appl. Polym. Sci.* 1995, **57**, 25
21 Kropp, L. J. and Dawson, R. W. 'Fluorescence and Phosphorescence of Aromatic Hydrocarbons in Polymethylmethacrylate', Molecular Luminescence Int. Conf. (Ed. C. C. Lim), Benjamin, New York, 1969
22 Bixon, M. and Jortner, J. *J. Chem. Phys.* 1968, **48**, 715